# Cyclodextrin-based Nanosponges for the Targeted Delivery of the Anti-restenotic Agent DB103: a Novel Opportunity for the Local Therapy of Vessels Wall Subjected to Percutaneous Intervention.

Vito Coviello,[ϛ^] Stefania Sartini,[ϛ^] Luca Quattrini,[ϛ] Cecilia Baraldi,[§] Maria Cristina Gamberini,[§] and Concettina La Motta.[ϛ*]

*Dipartimento di Farmacia, Università di Pisa, Via Bonanno 6, 56126 Pisa, Italy. Dipartimento di Scienze della Vita, Università degli Studi di Modena e Reggio Emilia, Via Giuseppe Campi 103, 41125, Modena, Italy.*

---

*To whom all correspondence should be addressed. C.L.M. Tel: (+)390502219593; e-mail: concettina.lamotta@unipi.it.

[^]These authors contributed equally to the work.

[ϛ]Dipartimento di Farmacia, Università di Pisa

[§]Dipartimento di Scienze della Vita, Università degli Studi di Modena e Reggio Emilia

## Abstract

Nano-sized colloidal carriers represent innovative drug delivery systems, as they allow a targeted and prolonged release of poorly water-soluble drugs, improving their bioavailability and modifying their pharmacokinetic parameters. In this work we describe cyclodextrin-based nanosponges, obtained through polimerization of β-cyclodextrin with diphenyl carbonate as the cross-linking agent, loaded with a novel multi-effective heterocyclic compound, **DB103**, able to regulate key cellular events involved in the remodelling of vessels wall. Fabrication and drug-loading procedures, as well as physical-chemical characterization and drug-release profile of the novel colloidal system are reported. Results achieved demonstrate the ability of nanosponges to enclose efficiently the target drug and release it slowly and continuously, thus suggesting the exploitability of the novel system for the local therapy of vessels wall subjected to percutaneous intervention.

## Keywords

β-cyclodextrin; β-cyclodextrin-based nanosponge; cardiovascular diseases; drug-eluting stent; 2-(3,4-dimethoxyphenyl)-3-phenyl-4*H*-pyrido[1,2-*a*]pyrimidin-4-one.

## Chemical compounds

β-cyclodextrin (PubChem CID: 70702285); diphenylcarbonate (PubChem CID: 7597); 2-(3,4-dimethoxyphenyl)-3-phenyl-4*H*-pyrido[1,2-*a*]pyrimidin-4-one (Scheme 1).

## Abbreviations

CVDs, cardiovascular diseases; PCI, percutaneous coronary intervention; DES, drug-eluting stent; **DB103**, 2-(3,4-dimethoxyphenyl)-3-phenyl-4*H*-pyrido[1,2-*a*]pyrimidin-4-one; NS, nanosponge; CD-NS, β-cyclodextrin-based nanosponges; DB103-NS, DB103-loaded nanosponges; ATR-FTIR, attenuated total reflectance-fourier transform infrared spectroscopy; DSC, differential scanning calorimetry; HAoSMCs, human aortic smooth muscle cells; HUVECs, human umbilical vein endothelial cells.

## 1. Introduction

Cardiovascular diseases (CVDs), represented by disorders of heart and blood vessels, are a major health problem in both developing and developed countries. Actually, besides being the main cause of morbidity worldwide, they represent the leading killer of men and women by 45 and 65 years of age, respectively, and are expected to be responsible for 23,3 million deaths by 2030 [1].

Most of CVDs are caused by atherosclerosis, a process of vessel wall degradation and calcification which leads to narrowing up to occlusion of blood vessels [2], thus requiring a percutaneous coronary intervention (PCI) [3]. Different techniques and devices have been developed to either remodel or remove the causes of acute and chronic vessel obstruction, increasing luminal cross-sectional area and improving blood flow. However, despite improvement in equipments, limitations still remain. Actually, patients may experience abrupt vessel closure at the treated site, as well as localized thrombus and vessel dissection. Moreover, recurrence of restenosis may affect up to 60% of patients, within 3 to 12 months after the treatment. Drug-eluting stents (DES) revamped the field of interventional cardiology, allowing to reduce the rate of restenosis and the need for repeated vascularization. However, some concerns still remain about their safety, particularly due to the rare but potentially life-threatening complication of in-stent thrombosis [4-6]. Inflammatory responses, local toxicity and allergic reactions may emerge to enhance restenosis and thrombosis, as a consequence of sub-optimal polymer biocompatibility. Actually, despite the success of DES, side effects to polymer coating still represent the main drawback of intra-vascular devices [7].

Accordingly, they need to be improved, and this results in an interesting field of research. In particular, more effective drugs should be identified, to be exploited for DES manufacturing, bearing in mind that the ideal therapeutic agent for vessel wall subjected to PCI should combine an anti-restenotic effect with a pro-healing action. Moreover, novel and more suitable drug carriers should be investigated as well, to promote endothelial healing through a controlled and predictable release of the effective drug in the targeted area avoiding any toxic side effects.

Pursuing our research interest in the field of CVDs treatments [8], we disclosed a novel multi-effective compound, namely 2-(3,4-dimethoxyphenyl)-3-phenyl-4*H*-pyrido[1,2-*a*]pyrimidin-4-one (**DB103**, Chart 1), which stood up as the ideal drug candidate for DES manufacturing [9-12].

Actually, our compound proved to inhibit human aortic smooth muscle cells (HAoSMCs) proliferation, responsible for the abnormal neointimal formation leading to restenosis. Moreover, in these cells, **DB103** inhibited also MMP-9 up-regulation and activity, which are induced by smooth muscle cell hyperplasia during atherosclerosis and restenosis to remodel the surrounding extracellular matrix [10]. In addition, it reduced the cytokine-induced expression of COX-2, followed by reduction of PGE2 production. On the contrary, in human umbilical vein endothelial cells (HUVECs), our drug candidate did not affect COX-2 protein and gene expression and did not modify the production of prostanoids, particularly the prostacyclin PGI2 which acts synergistically with nitric oxide to maintain normal vascular functions, i.e., atheroprotection, inhibition of platelet activation, and vascular smooth muscle contraction. Accordingly, **DB103** is able to regulate excellently key events involved in the remodelling of vessels wall.

Tested *ex-vivo* on platelet-rich plasma obtained from whole blood, **DB103** proved to counteract platelet aggregation induced by agonists such as collagen (5 μg/ml) and U46619 (1 μM), both involved in the TxA2 pathway, showing $IC_{50}$ values in the low micromolar range. It also inhibited platelet activation, as demonstrated by its ability to reduce the mean platelet component parameter, a measure of platelet density, sphering and swelling that correlates with the platelet activation state and can be easily determined exploiting the Advia 120 Hematology System [11].

Therefore, besides staking out restenosis, our compound may in principle prevents thrombotic events often coming on the scene of DES treatment.

However, to be exploited as the active pharmaceutical ingredient of DES, **DB103** should be incorporated within a suitable matrix, able to release it over time, slowly and safely. This is why we deepened our study, developing a promising and innovative system for drug delivery. In particular, we focussed on cyclodextrin-based nanosponges, obtained through polimerization of β-cyclodextrin

with diphenyl carbonate as the cross-linking agent. This hyper-cross-linked polymer is able to incorporate drugs within its structure, either as inclusion complexes or as non-inclusion complexes. Besides preserving drug stability, β-cyclodextrin nanosponges turn out to be fully bio-compatible, showing no cytotoxic and haemolytic activities [13]. Moreover, they can be easily sterilized, being thermally stable up to 300 °C. This carrier has already been exploited as a versatile drug delivery system [14-17], but it has never been investigated as an exploitable polymer for the controlled delivery of drug from DES, particularly for those equipped with reservoirs of drug carrying polymers [18]. Accordingly, it represents the best candidate for our study. In this work we describe the obtainment of the novel DB103-nanosponge system, which was fully characterized through physical-chemical data, and drug loading and releasing profile.

## 2. Experimental Section

**Materials and Methods.**

β-cyclodextrin, diphenylcarbonate, 2-aminopyridine, ethyl 3-(3,4-dimethoxyphenyl)-3-oxopropanoate, N-bromosuccinimide, bis(triphenylphosphine)palladium(II) dichloride, phenylboronic acid, and all other chemicals were from Sigma-Aldrich (St. Louis, MO). Melting point of **DB103** was determined using a Reichert Köfler hot-stage apparatus and it is uncorrected. Routine $^{1}$H-NMR spectra were recorded either in DMSO-$d_6$ (**DB103**) or in $D_2O$ solution (nanosponge and DB103-loaded nanosponges), on a Bruker 400 spectrometer operating at 400 MHz. Routine infrared spectra were obtained with an Agilent Cary 620 FT-IR Microscope Spectrometer.

**Chemical synthesis of DB103**

The target compound, 2-(3,4-dimethoxyphenyl)-3-phenyl-4*H*-pyrido[1,2-*a*]pyrimidin-4-one, namely **DB103**, was synthesized by V.C. and S.S. at the Department of Pharmacy of the University of Pisa, Italy, following the previously reported procedure depicted in Scheme 1 [11]. Briefly, the

key intermediate 2-(3,4-dimethoxyphenyl)-4*H*-pyrido[1,2-*a*]pyrimidin-4-one, **3**, obtained from 2-aminopyridine **1** and ethyl 3-(3,4-dimethoxyphenyl)-3-oxopropanoate **2** in polyphosphoric acid [19], was treated with N-bromosuccinimide in refluxing chloroform to afford the corresponding 3-bromo derivative, **4**, which gave the target **DB103** through reaction with phenylboronic acid in the presence of bis(triphenylphosphine)palladium(II) dichloride and an aqueous solution of $Na_2CO_3$, in EtOH/toluene solution. The crude product was purified by crystallization from MeOH, than anhydrified in a vacuum oven and characterized through physico-chemical and spectral data. Yield: 90%. P. f.: 182-184 °C. IR (ν, $cm^{-1}$): 1657, 1592, 1511, 1463, 1418, 1260, 1136, 1015. $^1$H-NMR (δ, ppm, Hz): 8.96 (d, 1H, J= 7.08), 7.95 (t, 1H, J=8.79), 7.73 (d, 1H, J=8.79), 7.34-7.10 (m, 7H), 6.88-6.75 (m, 2H), 3.72 (s, 3H), 3.36 (s, 3H).

**Chemical synthesis of β-cyclodextrin-based nanosponges (CD-NS)**

β-cyclodextrin nanosponges were synthesized following a previously reported procedure, devised by Trotta and co-workers [14] and depicted in Scheme 2. Briefly, a mixture of β-cyclodextrin, anhydrified in a vacuum oven (1.00 mmol) and diphenylcarbonate (4.00 mmol) were heated under stirring at 90 °C for 5 h. Once the reaction was completed, the solid cross-linked nanosponge was ground in a mortar and washed with water, to remove the unreacted β-cyclodextrin, then extracted with ethanol, to remove phenolic by-product and the residual diphenylcarbonate. The white product so obtained was anhydrified in a vacuum oven, then characterized through spectral data. IR (ν, $cm^{-1}$): 3316, 2927, 1773, 1648, 1229, 1153, 1026. $^1$H-NMR (δ, ppm, Hz): 4.98 (d, 1H, J= 3.68), 3.88 (t, 1H, J= 9.49), 3.79-3.76 (m, 3H), 3.59 (dd, 1H, J= 3.60, 9.93), 3.50 (t, 1H; J= 9.0).

**Preparation of DB103-loaded nanosponges (DB103-NS)**

The loaded nanosponges were prepared at a nanosponge:compound ratio of 1:1, w/w. Accordingly, 100.0 mg of CD-NS and 100.0 mg of **DB103** were dissolved in anhydrous DMF and left under stirring at room temperature for 1.0 hour. Then, the solvent was evaporated under reduced pressure and the resulting solid was washed with water and acetone, then anhydrified in a vacuum oven and

characterized through spectral data. IR (ν, $cm^{-1}$): 1658, 1627, 1593, 1512, 1463, 1417, 1324, 1234, 1137, 1017. $^{1}$H-NMR (δ, ppm, Hz): 7.84 (s, 1H), 7.21 (t, 1H, J=7.45), 6.81 (t, 1H, J=7.46), 6.79 (t, 1H, J=7.64), 4.98 (d, 1H, J=3.72), 3.86 (t, 1H, J=9.46), 3.78-3.73 (m, 3H), 3.57 (dd, 1H, J=3.66, J=9.94), 3.52 (t, 1H, J=9.60), 2.92 (s, 3H), 2.77 (s, 3H).

**Preparation of binary mixture of DB103 and nanosponges**

A binary physical mixture of test compound, **DB103**, and nanosponges was prepared by mixing, in a glass mortar and in a 1:1 weight ratio, appropriate amounts of the two solid components.

**UV spectral analysis of DB103**

2 mg of **DB103** were dissolved in 10 mL of ethanol and the resulting solution was scanned on a Perkin Elmer UV-Vis Spectrophotometer Lambda 25, between 200 and 400 nm, to determine the wavelength of maximum absorbance of the test compound. This latter, established at 318 nm, was exploited in the following loading and releasing studies.

**Attenuated Total Reflectance-Fourier transform infrared spectroscopy (ATR-FTIR)**

ATR-FTIR spectra of **DB103**, β-cyclodextrin-based nanosponge (CD-NS), their 1:1 physical mixture and DB103-loaded nanosponge (DB103-NS) were recorded on a FTIR Cary 620 microscope spectrometer using a micro ATR slide accessory with a Germanium crystal, in the region ranging from 3500 to 950 $cm^{-1}$. Chemical imaging data were collected on a 620 FTIR imaging system with a 64x64 Focal Plane Array (FPA) detector cooled by liquid nitrogen, utilizing Agilent's ATR-Imaging technique (Figures 1-4). Experimental parameters exploited for data processing are shown in Table 1.

**Differential scanning calorimetry (DSC)**

The thermal behaviour of **DB103** and DB103-loaded nanosponge (DB103-NS) were studied using a Perkin Elmer Pyris 6 DSC instrument under dry nitrogen purge. Samples were scanned at the rate of 10 °C/min, over the 45-280 °C temperature range. The instrument was calibrated with an indium sample (99.99% pure), having a melting point of 156.6 °C and a melting enthalpy of 28.4 J/g. The

Pyris Manager software was used to extrapolate onset value temperatures and melting enthalpy for each thermal event. Thermograms obtained are reported in Figure 7.

**Raman spettroscopy**

The Raman spectra of **DB103** and DB103-loaded nanosponge (DB103-NS) were recorded with a confocal Labram instrument (Jobin Yvon Horiba) equipped with a He-Ne laser at 632.8 nm and a CCD detector (254x1024), cooled by Peltier effect. Spectra were recorded in backscattering after focalisation in several positions within a small area of the sample (ca. 100 μm x 100 μm). The maximum laser power employed was 5 mW and the recording time for good signal-to-noise ratio was 100-200 s. GRAMS/AI 7.02 was used for the elaboration of the spectra, which are reported in Figure 8.

**Loading efficiency and loading capacity**

The loading efficiency and capacity of the DB103-NS system was determined spectrophotometrically on 2 mg of powder, accurately weighted, which was suspended in 10 mL of ethanol and sonicated for 10 minutes, to break the loaded nanosponge. The resulting solution was filtered, then suitably diluted and analysed by UV at 318 nm. Experiments were performed in triplicate and the loading efficiency and capacity were calculated by the following formulae (1) and (2),[20] respectively, converting the observed absorbance into mass (μg) by the use of a suitable calibration curve:

Loading Efficiency = (Effective Drug Content/Theoretical Drug Content) x 100 (1)

Loading Capacity = (Effective Drug Content/DB103-NS System Mass) x 100 (2)

**In vitro releasing studies**

Drug releasing from DB103-loaded nanosponge (DB103-NS) was monitored by UV spectroscopy. The loaded carrier, 2 mg, was placed in a 10.0 mL dissolution vessel and kept under stirring, at 37°C, in PBS solution. At selected time-points, 1.00 mL of solution was removed from the flask and replaced with 1.00 mL of fresh PBS, to maintain sink conditions. Collected samples were analysed by using Perkin Elmer UV-Vis Spectrophotometer Lambda 25. Selected time-points were:

0 min, 30 min, 1 h, 2 h, 3 h, 4 h, 6 h, 24 h and 48 h. The absorbance observed at 318 nm was converted into mass (μg) by using a suitable calibration curve. Blank measures (PBS) were used as the negative controls. Experiments were performed in triplicate and cumulative percentage of drug eluted with time, expressed as means±SEM, are reported in Figure 9.

## 3. Results and Discussion

Nanosponges are a new type of fully biocompatible cross-linked polymer endowed with great encapsulation ability and high solubilization capacity with regard to different types of molecules [13,14,20-30]. As their production is flexible and cost-effective, they represent a useful and innovative tool whose employment in drug delivery should be increased. In this study, we investigate the use of nanosponges for the obtainment of a novel system enclosing the multi-effective heterocyclic compound **DB103**, able to regulate key cellular events involved in the remodelling of vessels wall.

Firstly, following the previously reported procedure of Trotta and co-workers [14], we synthesized the carrier from β-cyclodextrin and diphenylcarbonate, obtaining a white pure matrix, consisting of a spherical shape nanoparticle population characterized by a narrow sizes distribution (data not shown). Once characterized through spectral data (Figures 2 and 5), nanosponges were then exploited to prepare the novel BD103-NS system, characterized in turn (Figures 4 and 6). Both nanosponges and BD103-NS system can be easily dispersed in water, giving rise to opalescent and stable colloidal suspensions [14]. Avoiding a gradient of concentration in the volume and guaranteeing equal excitation of the nuclei within the spectral range, these nano-sized systems may be easily analyzed through $^{1}$H-NMR data without using magic angle spinning conditions. The size of the particles are small enough to allow their incoherent isotropic tumbling motions, and both dipolar coupling and chemical shift anisotropy can be eliminated. Moreover, brownian motions help to sharpen the signal of the colloidal particles and of the adsorbed compound [31-33].

Once loaded with the active compound, nanosponges changed their $^{1}$H-NMR spectrum, as can be easily deduced comparing Figures 5 and 6. Chemical shifts pertaining to protons H-1 (δ=4.98), H-2 (δ=3.56), and H-6 (δ=3.79) of the carrier, protruding outside the cavity, were almost unaffected by complexation but those related to protons H-3 and H-5, located inside the carrier cavity, showed an upfield shifting ranging from 0.019 to 0.035 ppm, thus confirming an inclusion complexation between nanosponges and the guest drug. Proton H-4 (δ=3.50 in the unloaded carrier) was affected too, and the 0.02 ppm downfield shifting observed in the loaded nanosponges corroborates the tight interaction between the carrier and **DB103**. Regarding this latter, the $^{1}$H-NMR spectrum was significantly biased upon loading on nanosponges. Indeed, in the DB103-NS system, both the aromatic protons and the alkyl protons of the dimethoxy substituents were shifted upfield by 0.50 to 1.12 ppm.

The novel BD103-NS system was then studied in depth, to ascertain its physicochemical characteristics and investigate both the loading efficiency/capacity and the ability to release the loaded drug.

**ATR-FTIR Studies.** Infrared spectroscopy was used to estimate interactions between nanosponge and the guest molecule in the solid state. Spectra of both the BD103-NS system and of the single components, as well as of the binary physical mixture of **DB103** and NS, were registered exploiting the ATR-FTIR, a profitable technique allowing high resolution images, short times data collections, high spatial resolution with high signal-to-noise ratio, and full information about the entire sample [34]. Thanks to the use of a Focal Plane Array Detector (FPA), which works as a camera, it is possible to collect simultaneously spectra from each single pixel of the image, giving a univocal IR per point, analyzing an area of 1.1 μm$^{2}$.

Figure 1 shows the ATR-FTIR spectrum and the visible and FPA images (2D and 3D in false colors) of **DB103**. Distinctive bands of **DB103** were found at 1657 cm$^{-1}$, due to C=O stretching, 1511 cm$^{-1}$, due to C=N stretching of aromatic ring, 1463 cm$^{-1}$, due to $CH_3$ bending vibration, 1260 cm$^{-1}$, due to the asymmetric stretching of C-O-C, and 1015 cm$^{-1}$, due to the symmetric stretching of

C-O-C. ATR-FTIR spectrum of plain cyclodextrin-nanosponges, reported in Figure 2, showed typical bands at 3316 $cm^{-1}$, due to O-H stretching, 2927 $cm^{-1}$, due to C-H stretching vibration, 1773 $cm^{-1}$, due to the presence of the carbonyl cross-linker, and 1026 $cm^{-1}$, due to C-O stretching of primary alcohol, thus proving to match fully IR data described by the literature for this nanocarrier [20].

The binary physical mixture DB103-nanosponge, analyzed by ATR-FTIR, provided the spectrum reported in Figure 3, which turned out to be the mere superimposition of the spectra registered for the single components, **DB103** and NS. Indeed, neither shifts nor modifications of the absorption bands were observed, thus demonstrating the absence of significant interactions between the nanosponge and the drug composing the mixture.

On the contrary, significant shifts of distinctive bands to higher frequencies were observed in the ATR-FTIR spectrum of the DB103-NS system, depicted in Figure 4, as a result of complexation between the nanosponge and the guest drug. The main stretching due to the C=O bond of **DB103** turned out to be shifted, from 1657 $cm^{-1}$ to 1688 $cm^{-1}$. The same was also true for the asymmetric stretching of C-O-C, from 1260 $cm^{-1}$ to 1272 $cm^{-1}$. Moreover, bands at 3292 $cm^{-1}$ and 2979 $cm^{-1}$, due to O-H and C-H stretching vibration of nanosponges, respectively, changed their shape and their intensity. Finally, stretching at 1026 $cm^{-1}$, due to C-O of primary alcohol, shifted to 1037 $cm^{-1}$ in the solid system.

**DSC Studies.** Figure 7 represents the DSC thermograms of **DB103** and DB103-NS system. The thermogram of the pure heterocyclic compound exhibited mainly a double endotherm peak, at 165 and 175 °C respectively, accompanied by a small and broad peak at 100 °C due to water traces. On the contrary, when the compound is complexed with the nanosponge, we assist to a substantial reduction in the endotherm peak intensity and a shift to lower temperatures: the double distinctive peak of **DB103** has been replaced by a single broad event, at 164 °C. Moreover, the thermogram of the DB103-NS system displayed an additional broad peak, at 79 °C. Both the events confirm the occurrence of a complex phenomenon between the two components.

**Raman Spectroscopy Studies.** As Raman spectroscopy is a key technique for studying interactions between drugs and polymers, we registered and compared Raman spectra of **DB103** and DB103-NS system. Results obtained are showed in Figure 8. Key peaks of **DB103**, highlighted in the upper spectrum, turned out to be either splitted or displaced in the spectrum of DB103-NS system. Actually, in this latter, additional peaks at 1600, 1330, and 650 $cm^{-1}$, due to the vibrational absorptions of the heterocyclic ring, are clearly visible, thus demonstrating that a close complex has been formed between the pyridopyrimidinone core and the network of β-cyclodextrins.

**Drug loading efficiency and drug loading capacity.** The amount of **DB103** loaded on the nanosponge was determined spectrophotometrically on a fixed amount of powder. Exploiting a suitable calibration curve, and using the previously mentioned formulae, the calculated percent of drug loading efficiency turned out to be 95±16 while the drug loading capacity resulted 35.6±8. It is known that the degree of cross-linking chosen in the manufacturing of nanosponges affects the complexation capacity of the carrier, as it modulates the size of the tridimensional network hosting the drug [35]. The 1:4 molar ratio between β-cyclodextrin and diphenylcarbonate pursued in our study guarantees a profitable interaction of **DB103** with the cavities of the nanosponge, as the percent of both drug loading efficiency and capacity resulted highly favorable.

**Drug releasing profile**. The releasing profile of **DB103** from the DB103-NS system was investigated in PBS solution and evaluated at specified time intervals, covering a time-span of 48 hours. Results obtained, reported as the cumulative percentage of drug released as a function of time, are plotted in Figure 9. **DB103** is released slowly and steadily, as less than 50% drug release was achieved over 48 hours of observation. The in vitro release profile was biphasic. A limited initial burst release, due to surface associated drug and represented by less than 10% loaded drug up to 0.5 hour, is then followed by a slow and sustained release phase, in which the entrapped drug slowly diffused into the release medium. The observed releasing profile confirms the good complexation and the strong interaction between the drug and the nanosponge network.

Since the DB103-NS system has been designed for the controlled delivery of drug from DES, the observed releasing profile turns out to be particularly convenient, as it allows a constant therapeutic effect minimizing potential toxicities.

## 4. Conclusions

Manufacturing of DES represents a challenging field of research. Despite their widespread use in interventional cardiology, these devices still presents some drawbacks, pertaining to both the drug and the carrier exploited in their fabrication. Actually, while the former should limit the growth of excess neointimal hyperplasia without preventing ultimate re-endothelialization of the stented artery, the latter should promote endothelial healing through a controlled release of the drug, avoiding any toxic side effects. In this work we presented a novel prototype candidate for DES manufacturing, obtained by combining a multi-effective compound, **DB103** [9], with an innovative carrier, represented by cross-linked, β-cyclodextrin-based nanosponges.

Although already exploited to increase drug solubility and bioavailability [36], the colloidal nanocarrier here proposed has never been proposed for DES manufacturing, particularly those equipped with reservoirs of drug carrying polymers [18].

However, being fully bio-compatible and devoid of any cytotoxic and haemolytic activities [13], β-cyclodextrin-based nanosponges may represent the ideal support to exploit in cutting-edge DES, as they allow to overcome in principle side effects arising from the coating polymer currently used [7].

The novel DB103-NS system was characterized through physico-chemical data, which demonstrated a clear and high grade inclusion of the active compound within the network of the nanosponge. In vitro release studies revealed the ability of the system to retain and release the active compound slowly and gradually, without any significant initial burst effect, thus assuring in principle an enduring therapeutic action at the site of intervention. Accordingly, the DB103-NS

system here described represent an innovative and reliable prototype of formulation exploitable for the local therapy of vessels wall subjected to percutaneous intervention.

## Acknowledgements

This work was supported by the Fondazione Pisa, within the framework of the Micro-VAST project (Grant 153/09, www.microvast.it).

### Conflict of Interest Disclosure

The authors declare neither financial nor personal conflicts of interest.

## References

1. Lim, G. B. Public health: quantifying the global burden of ischaemic heart disease. *Nature Reviews Cardiology*. **2014**, 11, 248.
2. Libby, P. Inflammation in atherosclerosis. *Nature*. **2002**, *420*, 868-874.
3. Hlatky, M. A.; Boothroyd, D. B.; Baker, L. C.; Go, A. S. Impact of drug-eluting stents on the comparative effectiveness of coronary artery bypass surgery and percutaneous coronary intervention. *Am. Heart J.* **2015**, *169*, 149-154.
4. Ishikawa, K.; Aoyama, Y.; Hirayama, H. Management of drug-eluting stent restenosis. *J. Invasive Cardiol.* **2012**, *24*, 178-182.
5. Garg, S.; Serruys, P. W. Coronary stents: current status. *J Am. Coll. Cardiol.* **2010**, *56*, 1-42.
6. Costa, M. A.; Simon, D. I. Molecular basis of restenosis and drug-eluting stents. *Circulation*. **2005**, *111*, 2257-2273.
7. Montone, R.; Sabato, V.; Sgueglia, G.; Niccoli, G. Inflammatory mechanisms of adverse reactions to drug-eluting stents. *Curr. Vasc. Pharmacol.* **2013**, *11*, 392-398.

8. Sartini, S.; Cosconati, S.; Marinelli, L.; Barresi, E.; Di Maro, S.; Simorini, F.; Taliani, S.; Salerno, S., Marini, A. M., Da Settimo, F.; Novellino, E.; La Motta, C. Benzofuroxane derivatives as multi-effective agents for the treatment of cardiovascular diabetic complications. Synthesis, functional evaluation, and molecular modeling studies. *J. Med. Chem.* **2012**, *55*, 10523-10531.
9. La Motta, C.; Da Settimo F.; Dario B.; Sartini S.; Basta G.; Del Turco S.; and Saponaro C. Therapeutic agent for treatment of blood vessels. PCT Int. Appl. WO2013144860.
10. Del Turco, S.; Sartini, S.; Sentieri, C.; Saponaro, C.; Navarra, T.; Dario, B.; Da Settimo, F.; La Motta, C.; Basta, G. A novel 2,3-diphenylpyrido[1,2-*a*]pyrimidin-4-one derivative inhibits endothelial cell dysfunction and smooth muscle cell proliferation/activation. *Eur J Med Chem*. **2014**, *72*, 102-109.
11. Del Turco, S.; Sartini, S.; Cigni, G.; Sentieri, C.; Sbrana, S.; Battaglia, D.; Papa, A.; Da Settimo, F.; La Motta, C.; Basta, G. Synthetic analogues of flavonoids with improved activity against platelet activation and aggregation as novel prototypes of food supplements. *Food Chemistry*. **2015**, *175*, 494-499.
12. Vannozzi, L.; Ricotti, L.; Filippeschi, C.; Sartini, S.; Coviello, V.; Piazza, V.; Pingue, P.; La Motta, C.; Dario, P.; Menciassi, A. Nanostructured ultra-thin patches for ultrasound-modulated delivery of anti-restenotic drug. *Int J Nanomedicine*. **2015**, 11, 69-91.
13. Shende, P.; Kulkarni, Y. A.; Gaud, R. S.; Deshmukh, K.; Cavalli, R.; Trotta, F.; Caldera, F. Acute and repeated dose toxicity studies of different β-cyclodextrin-based nanosponge formulations. *J Pharm Sci.* **2015**, 104, 1856-63.
14. Trotta, F.; Zanetti, M.; Cavalli, R. Cyclodextrin-based nanosponges as drug carriers. *Beilstein J. Org. Chem.* **2012**, *8*, 2091–2099.
15. Tejashri, G.; Amrita, B.; Darshana, J. Cyclodextrin based nanosponges for pharmaceutical use: a review. *Acta Pharm.* **2013**, *63*, 335-358.

16. Wolfram, J.; Zhu, M.; Yang, Y.; Shen, J.; Gentile, E.; Paolino, D.; Fresta, M.; Nie, G.; Chen, C.; Shen, H.; Ferrari, M.; Zhao, Y. Safety of Nanoparticles in Medicine. *Curr. Drug Targets*. **2014** Aug 4.
17. Chilajwar, S. V.; Pednekar, P. P.; Jadhav, K. R.; Gupta, G. J.; Kadam, V. J. Cyclodextrin-based nanosponges: a propitious platform for enhancing drug delivery. *Exp. Opin. Drug Delivery*. **2014**, *11*, 111-120.
18. Abizaid, A.; Ribamar Costa, Jr J. New Drug-Eluting Stents. An overview on biodegradable and polymer-free next-generation stent systems. *Circulation: Cardiovascular Interventions*. **2010**, *3*, 384-393.
19. La Motta, C.; Sartini, S.; Mugnaini, L.; Simorini, F.; Taliani, S.; Salerno, S.; Marini, A. M.; Da Settimo, F.; Lavecchia, A.; Novellino, E.; Cantore, M.; Failli, P.; and Ciuffi, M. Pyrido[1,2-*a*]pyrimidin-4-one derivatives as a novel class of selective aldose reductase inhibitors exhibiting antioxidant activity. *J. Med. Chem.* **2007**, *50*, 4917-27.
20. Ankrum, J. A.; Miranda, O. R.; Ng, K. S.; Sarkar, D.; Xu, C.; Karp, J. M. Engineering cells with intracellular agent–loaded microparticles to control cell phenotype. *Nature Protocols*. **2014**, *9*, 233-245.
21. Trotta, F.; Cavalli, R. Characterization and applications of new hyper-cross-linked cyclodextrins. *Composite Interfaces*. **2009**, *16*, 39-48.
22. Rekharsky, M. V.; Inoue, Y. Complexation thermodynamics of cyclodextrins, *Chem. Rev.* **1998**, *98*, 1875-1917.
23. Mihailiasa, M.; Caldera, F.; Li, J.; Peila, R.; Ferri, A.; Trotta, F. Preparation of functionalized cotton fabrics by means of melatonin loaded β-cyclodextrins nanosponges. *Carbohydrate Polymers*. **2016**, *142*, 24-30.
24. Shivani, S.; Poladi, K. K. Nanosponges, novel emerging drug delivery system: a review. *Int. J. Pharm. Sci. Res.* **2015**, *6*, 529-540.

25. Coupland, J. N.; Hayes, J. E. Physical approaches to masking bitter taste: lessons from food and pharmaceutical. *Pharm. Res.* **2014**, *31*, 2921-2939.
26. Paolino, M.; Enne, F.; Lamponi, S.; Cernescu, M.; Voit, B.; Cappelli, A.; Appelhans, D.; Komer, H. Cyclodextrin-adamantane host-guest interactions on the surface of biocompatible adamantyl-modified glycodendrimers. *Macromolecules*. **2013**, *46*, 3215-3227.
27. Osmani, R. A.; Hani, U.; Bhosale, R. R.; Kulkarni, P. K.; Shanmuganathan, S. Nanosponge carriers - an archetype swing in cancer therapy: a comprehensive review. *Curr Drug Targets*. **2017**, *18*, 108-118.
28. Hayiyana, Z.; Choonara, Y. E.; Makgotloe, A.; du Toit, L. C.; Kumar, P.; Pillay, V. Ester-based hydrophilic cyclodextrin nanosponges for topical ocular drug delivery. *Curr. Pharm. Des*. **2016**, *22*, 6988-6997.
29. Trotta, F.; Caldera, F.; Cavalli, R.; Soster, M.; Riedo, C.; Biasizzo, M.; Uccello Barretta, G.; Balzano, F.; Brunella, V. Molecularly imprinted cyclodextrin nanosponges for the controlled delivery of L-DOPA: perspectives for the treatment of Parkinson's disease. *Expert Opin. Drug Deliv*. **2016**, *13*, 1671-1680.
30. Conte, C.; Caldera, F.; Catanzano, O.; D'Angelo, I.; Ungaro, F.; Miro, A.; Pellosi, D. S.; Trotta, F.; Quaglia, F. β-cyclodextrin nanosponges as multifunctional ingredient in water-containing semisolid formulations for skin delivery. *J. Pharm. Sci*. **2014**, *103*, 3941-3949.
31. Kazarian, S. G.; Chan, K. L. A. "Chemical Photography" of drug release. *Macromolecules*. **2003**, *36*, 9866-9872.
32. Schwarz, J.A., Contescu C.I., Surface of nanoparticles and porous material, CRC Press, 1999.
33. Andrieux, D., Jestin, J., Kervarec, N., Pichon, R., Privat, M., Olier, R. Adsorption mechanism of substituted pyridines on silica suspensions: an NMR study. *Langmuir*. **2004**, *20*, 10591-10598.
34. Yesinowski, J.P. High-resolution NMR spectroscopy of solids and surface-adsorbed species in colloidal suspension: phosphorus-31 NMR spectra of hydroxyapatite and diphosphonates. *J. Am. Chem. Soc*. **1981**, *103*, 6266-6267.

35. Kazarian, S. G.; Chan, K. L. A. Applications of ATR-FTIR spectroscopic imaging to biomedical samples. *Biochim. Biophys. Acta*. **2006**, *1758*, 858-867.
36. Singireddy A.; Subramanian, S. Fabrication of cyclodextrin nanosponges for quercetin delivery: physicochemical characterization, photostability, and antioxidant effects. *J. Mater. Sci*. **2014**, *49*, 8140-8153.
37. Dora, C. P.; Trotta, F.; Kushwah, V.; Devasari, N.; Singh, C.; Suresh, S.; Jain, S. Potential of erlotinib cyclodextrin nanosponge complex to enhance solubility, dissolution rate, in vitro cytotoxicity and oral bioavailability. *Carbohydr Polym*. **2016**, 137, 339-49.

**Figure 1.** ATR-FTIR spectrum, visible and FPA images (2D and 3D in false colors) of **DB103**

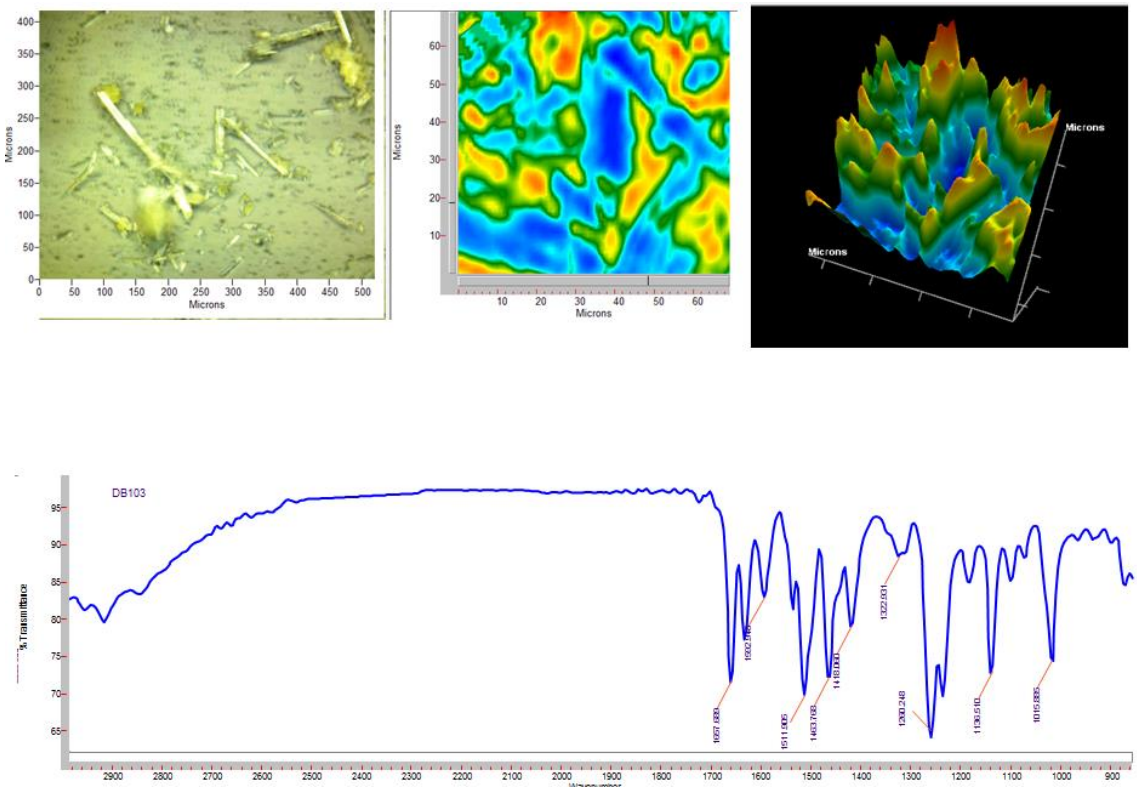

**Figure 2.** ATR-FTIR spectrum, visible and FPA images (2D and 3D in false colors) of nanosponges.

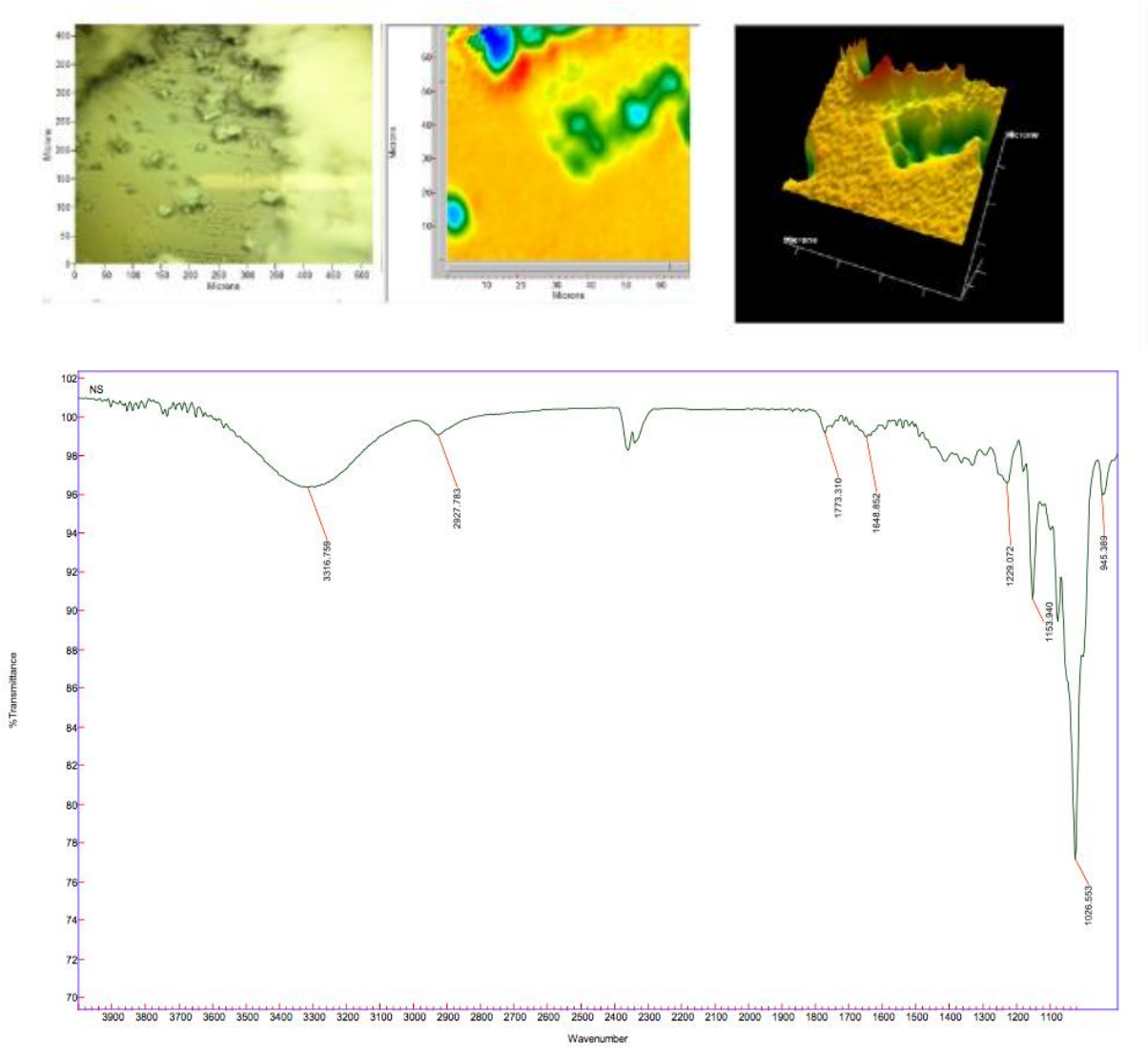

**Figure 3.** ATR-FTIR spectrum, visible and FPA images (2D and 3D in false colors) of the binary physical mixture of **DB103** and nanosponges.

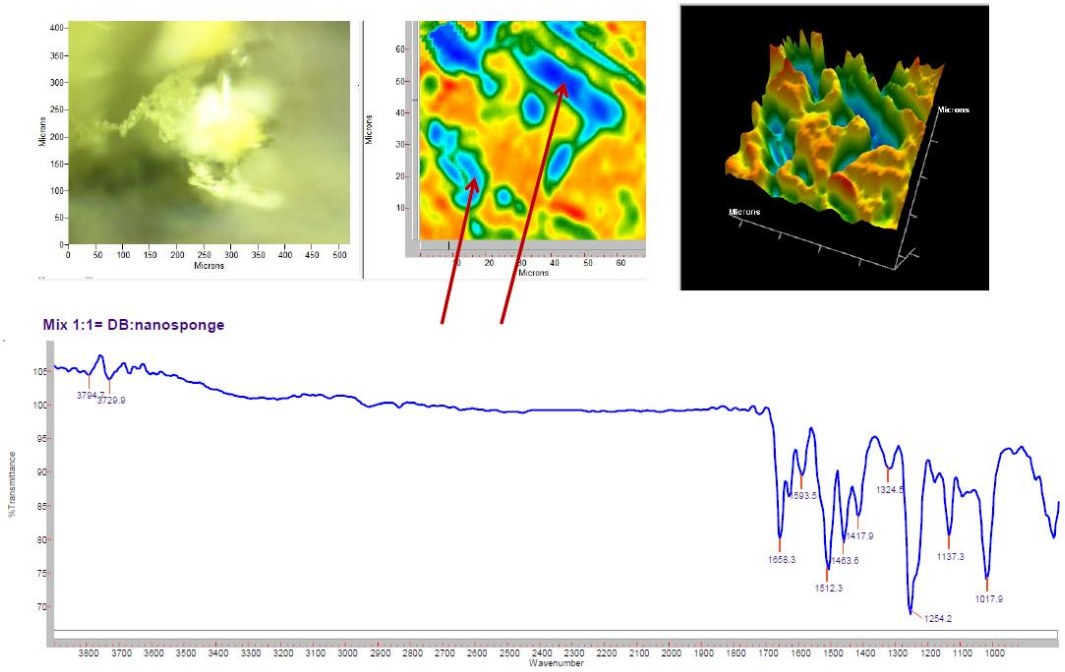

**Figure 4.** ATR-FTIR spectrum, visible and FPA images (2D and 3D in false colors) of DB103-NS system.

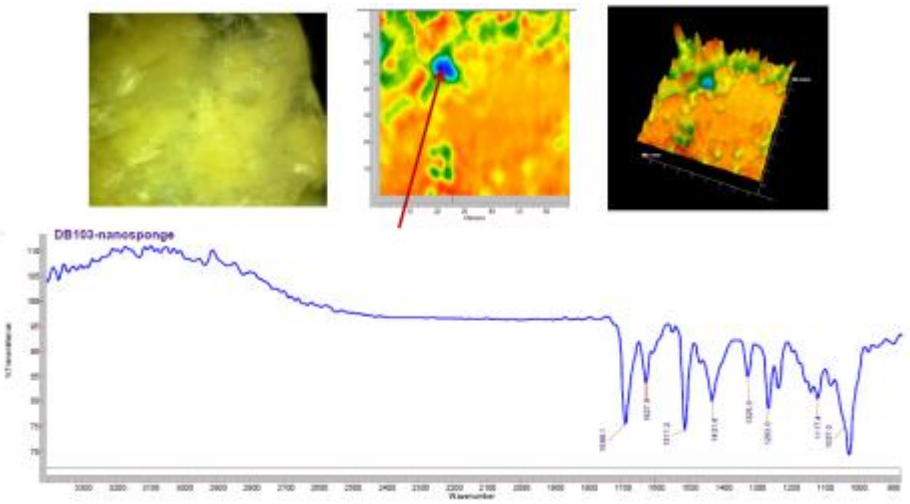

**Figure 5.** $^{1}$H-NMR Spectrum of β-Cyclodextrin-based Nanosponges, recorded in $D_2O$.

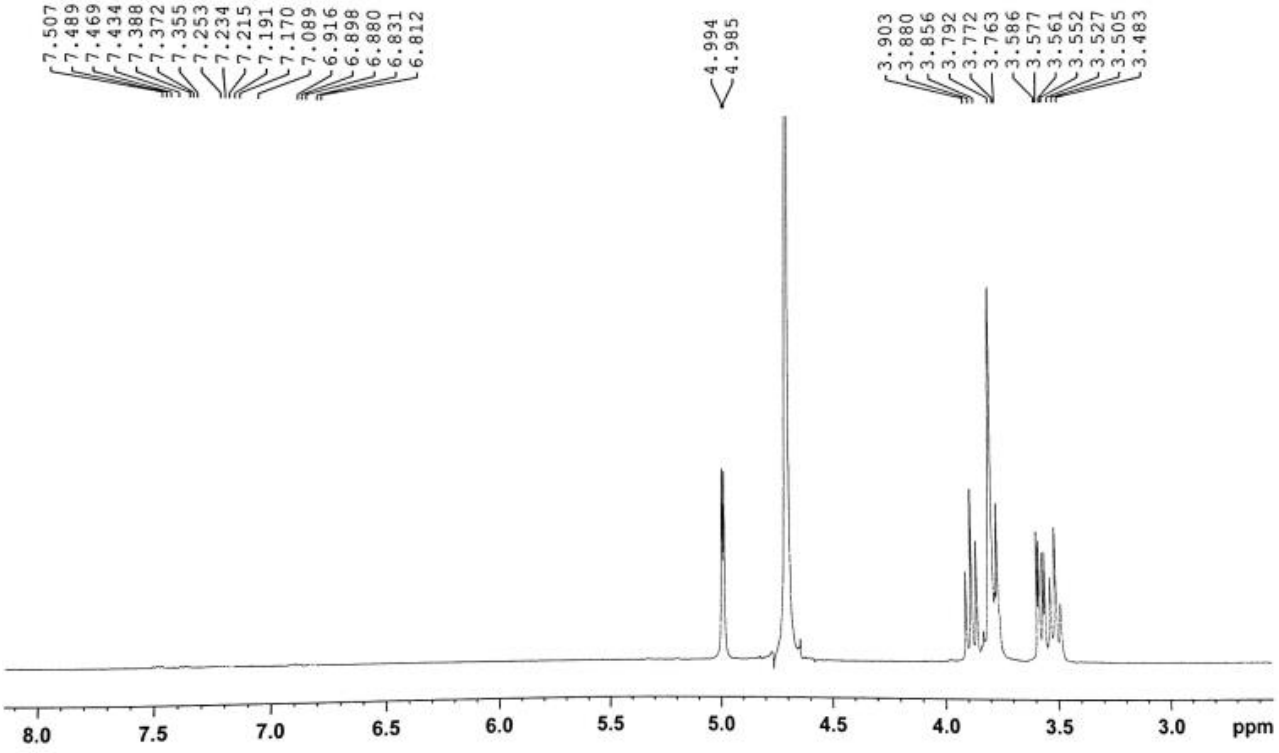

**Figure 6.** $^{1}$H-NMR Spectrum of DB103-NS System, recorded in $D_2O$.

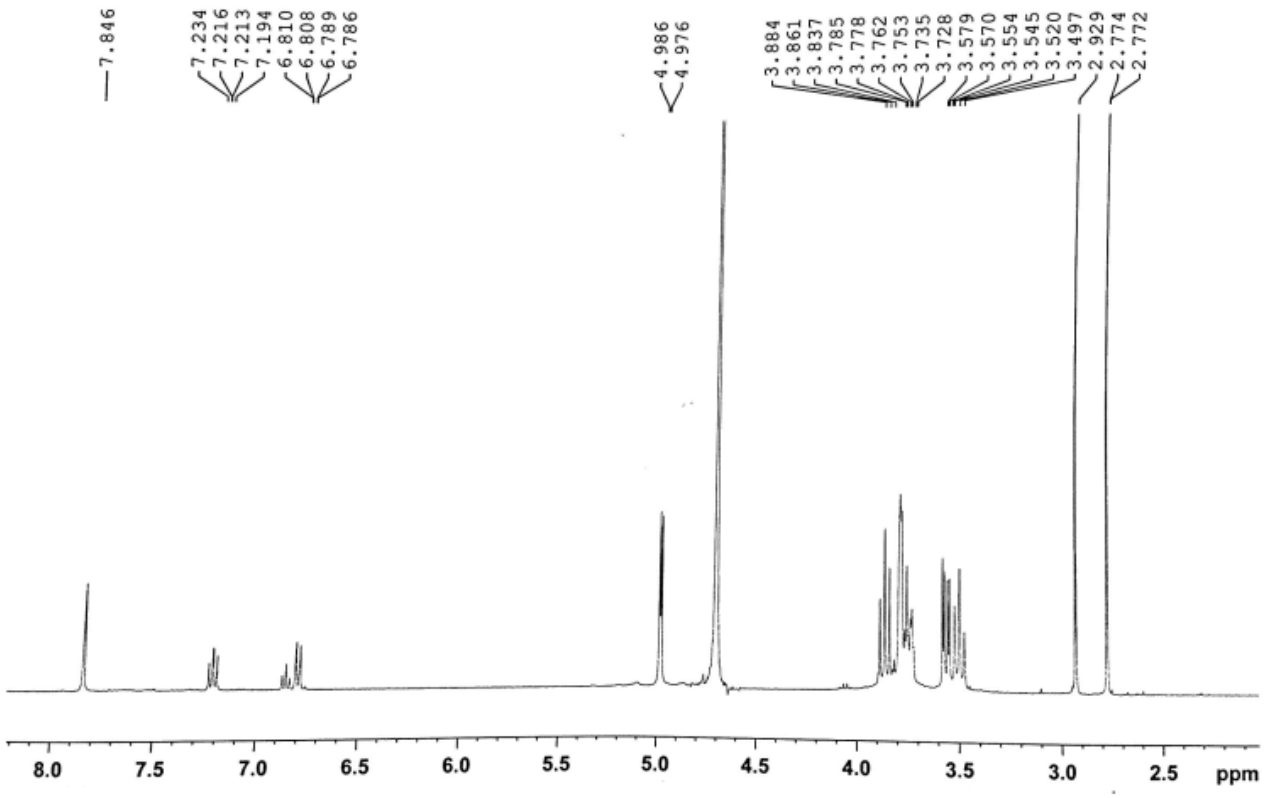

**Figure 7.** DSC Thermograms of **DB103** (black line) and DB103-NS System (red line).

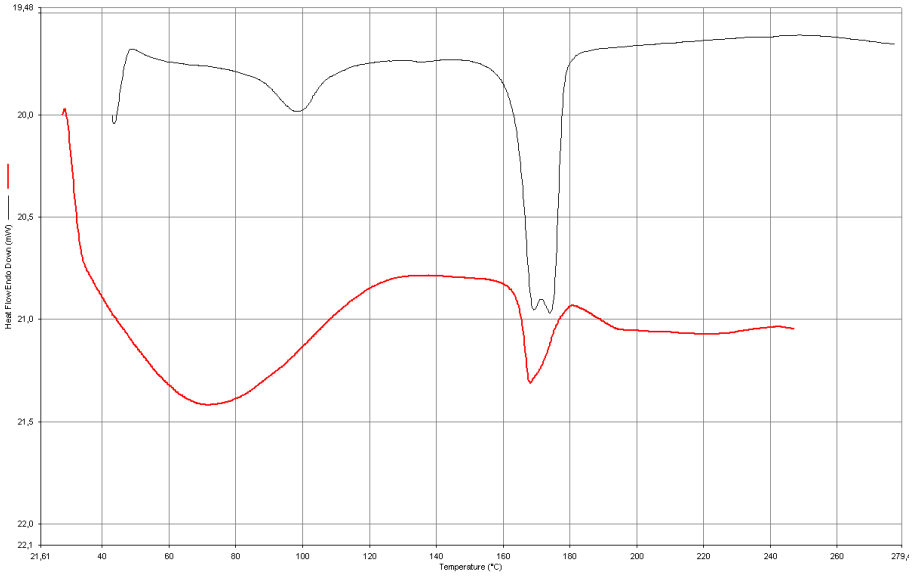

**Figure 8.** Raman Spectra of **DB103** and DB103-NS System.

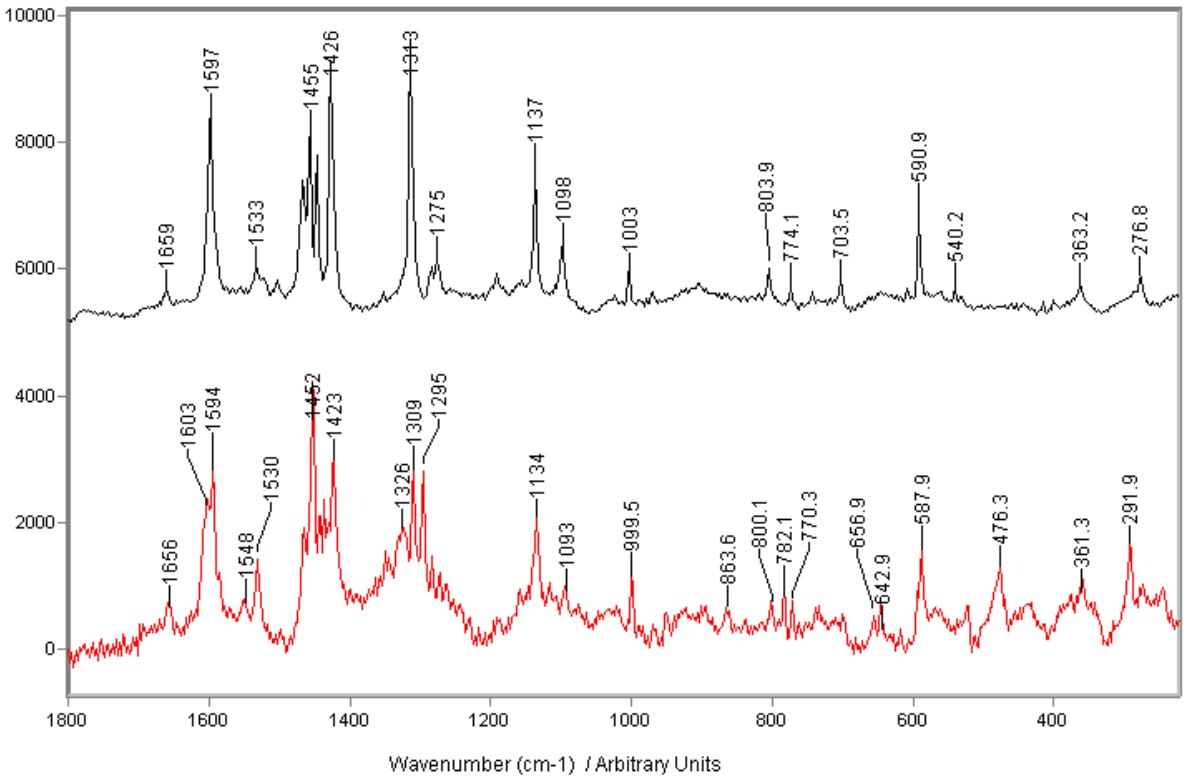

**Figure 9.** In Vitro Drug Releasing Profile of DB103-NS System.

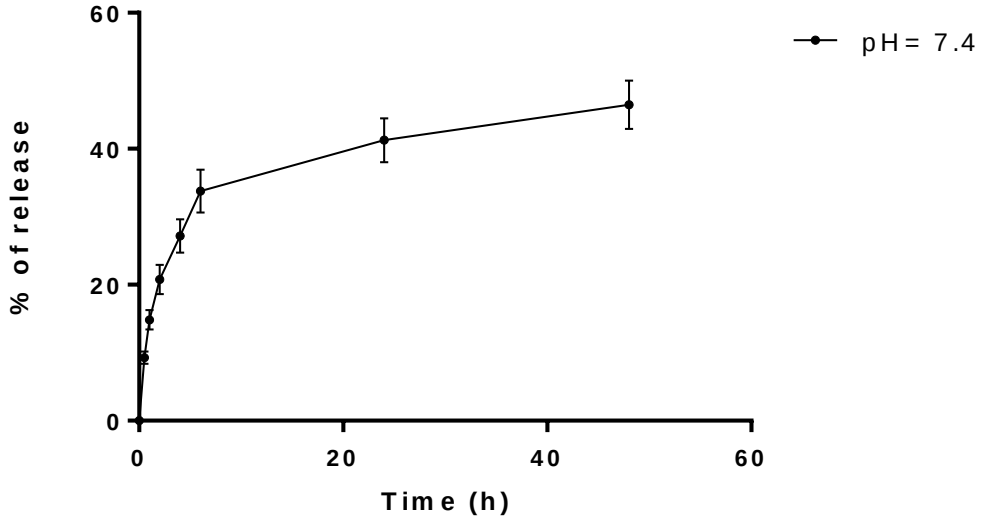

**Scheme 1**. Chemical Synthesis of **DB103**.

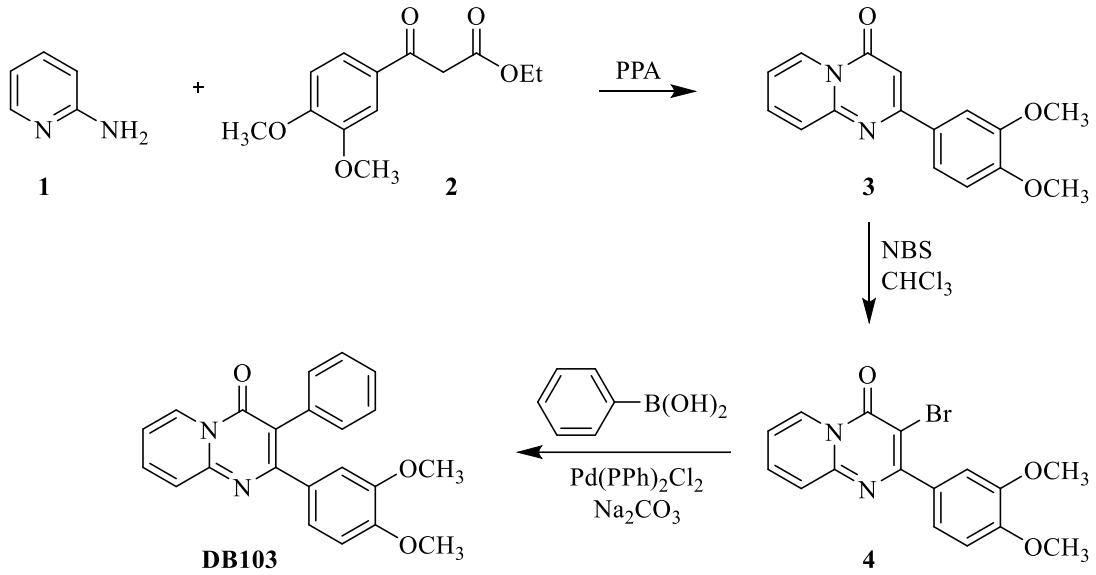

**Scheme 2.** Chemical Synthesis of β-Cyclodextrin-based Nanosponges

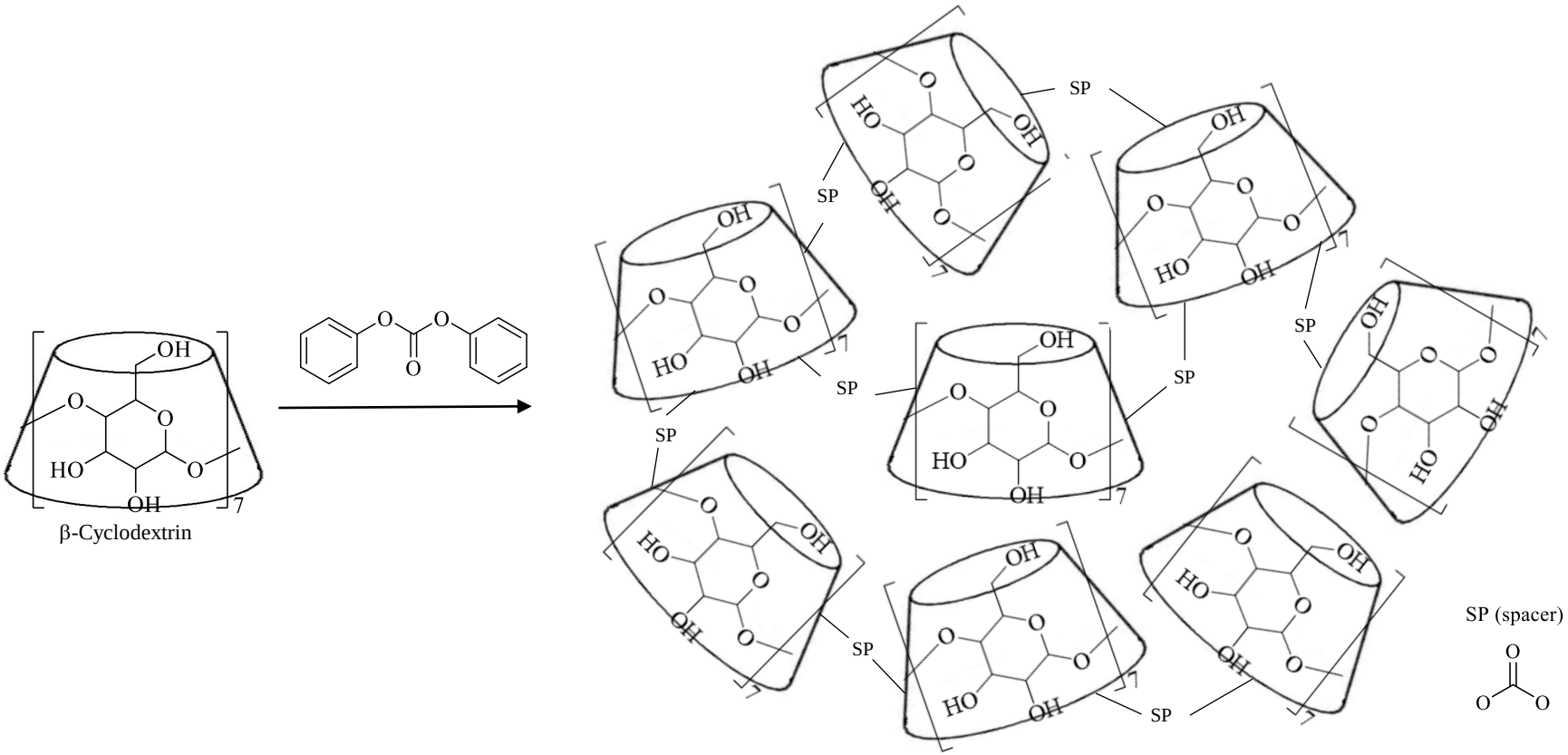

**Table 1.** Experimental Parameters of ATR-FTIR Study.

| Parameter | Value |
|---|---|
| Number of background scans | 256 |
| Number of sample scans | 256 |
| Spectral resolution ($cm^{-1}$) | 8 |
| Speed (KHz/sec) | 2.5 |
| Aperture ($cm^{-1}$) | 4 |
| Post processing | Principal component analysis (PCA) $CO_2$ and $H_2O$ subtraction |